International Journal of Control, Automation and Systems 16(4) (2018) 1724-1735
http://dx.doi.org/10.1007/s12555-016-0784-1
ISSN:1598-6446 eISSN:2005-4092
http://www.springer.com/12555

Guidance Laws against Towed Decoy Based on Adaptive Back-stepping Sliding Mode and Anti-saturation Methods

Ji-Peng Dong, Jing-Guang Sun, Yong Guo, and Shen-Min Song*

Abstract: In order to meet the needs of high-precision guidance for missile-guided maneuvering targets in the presence of towed bait interference, this paper proposes a new guidance strategy based on heading angle method and parallel approaching method. Its main idea: a suitable angle is determined by heading angle method which of the missile trajectory is above that of the towing bait. Meanwhile, the accurate interception of missiles to targets is guaranteed by parallel approaching method. Firstly, system models of missile and target with towed decoy are established. Then, considering unknown bounded system disturbances, a controller is given based on sliding mode, back-stepping method. Furthermore, to solve the input saturation problem, an anti-saturation controller is given using adaptive and back-stepping sliding mode methods. Finally, strict proofs of the two controllers are given using Lyapunov stability theory, and simulations are carried out to verify the effectiveness of the two controllers.

Keywords: Adaptive control, finite time control, guidance law design, terminal sliding mode control, towed decoy missile.

1. INTRODUCTION

With the fast development of electric jamming technology, the survival ability of the carrier is improved significantly [1]. As a new defensive jamming method, towed decoy plays an important strategic role in modern electronic countermeasure battle [2,3]]. And now towed decoy becomes an important means of countering radar seeker of anti-air missiles and has been applied in warfare successfully, which makes the anti-air missiles with radar seeker face severe challenges to intercept the carriers with towed decoys. Therefore, the research on terminal guidance laws with the ability of resistance of towed decoy has certain significance on the design of guidance laws against towed decoys.

The present literatures are focused on mechanism [4,5] and performance analysis of towed decoy jamming [6,7]. There are few studies on guidance laws against towed decoys. Since the dynamic properties of guidance system are complicated, the design method of the controller based on linear models is no longer suitable. Therefore many nonlinear control methods are widely applied in the field of the aircraft control. Since the sliding mode control theory is of good robustness to the inner parameter perturbations and outer disturbances of the system, which make it applied to guidance law design widely. In [8], the sliding mode method was firstly used to design the guidance law for air-to-air missiles. In order to deal with disturbances with unknown upper bounds, an adaptive technology was introduced in the controller design [9, 10]. In [9], an adaptive controller was proposed for linear time-invariant systems based on adaptive control technique. In [10], an adaptive second-order sliding mode output feedback controller was proposed for dynamical system with disturbances with unknown upper bounds. However, the adaptive parameters are not bounded. In [11–13], an adaptive nonsingular sliding mode guidance law was designed with impact angle constraints. In [14], the adaptive sliding mode guidance law was designed for the situation of interception of high-speed large maneuvering target. Since sign functions are contained in the guidance law, system chattering will be introduced. In order to address this problem, the adjustment of high-gain guidance parameters was realized by the guidance law based on intelligent control and sliding mode theory in [15], thus the chattering caused by sign functions will be eliminated. In addition, the delays may also cause chattering in sliding mode control systems [16, 17]. A sliding mode output feedback controller was designed for non-linear systemwhich can compensate the status and output delays in [17]. Com-

Manuscript received December 15, 2016; revised June 15, 2017 and October 27, 2017; accepted January 12, 2018. Recommended by Associate Editor Xiaojie Su under the direction of Editor Hamid Reza Karimi. This paper was supported by the National Natural Science Foundation of China under Grant 6117403, the State Key Program of National Natural Science of China under Grant 61333003, the Aeronautical Science Foundation of China under Grant 20140177002.

Ji-Peng Dong, Jing-Guang Sun, Yong Guo, and Shen-Min Song are with the Center for Control Theory and Guidance Technology, Harbin Institute of Technology, Harbin, 150001, China (e-mails: dongjipeng_hit@163.com, sunjingguanghit@163.com, guoyong@nwpu.edu, songshenmin@hit.edu.cn).
* Corresponding author.

pared to asymptotic stability guidance laws [14, 15], the guidance law which can realize convergence to an equilibrium point in finite time makes more theoretical and practical sense. The terminal sliding mode guidance law converging in finite time with impact angle constraint using terminal factors was proposed in [18]. But the controller has the singularity problem. To deal with the singularity problem, the finite time convergence guidance law with impact angle constraint was proposed in [19], based on non-singularity terminal sliding mode surface combined with expanded state observer. Some back-stepping controllers were proposed to have strong robustness in external disturbance and high precision in guidance law system [18, 20–23]. For example, some guidance laws with finite time convergence using integral back-stepping control method were proposed by considering the missile autopilot in [18, 20]. In [21], a three-dimensional guidance law was designed accounting for considering aerodynamic uncertainties, cross-coupling effects, model uncertainties and target maneuvers, based on second-order sliding mode and back-stepping technique. A back-stepping controller of integrated missile guidance and control system designed using active disturbance rejection control theory in [22]. In [23], an adaptive back-stepping controller was proposed for missile guidance and control system, which used the sliding mode theory and fuzzy theory.

In the actual control system design, input saturation problems must be considered [24–27]. An auxiliary system was formed and an adaptive dynamic surface controller was shown in [26] to solve the problem of input saturation of guidance control system. Not only the stability of the system was guaranteed, but also the satisfying interception performance was obtained. Dynamic surface controllers based on neural network were given in [26] to deal with the input saturation problem of a class of uncertain nonlinear systems. An adaptive dynamic surface controller was given in [27] by an auxiliary system to solve the three-dimension of guidance problem with input saturation in autopilot. Based on back-stepping sliding mode method and auxiliary system, the guidance law to deal with uncertainty and input saturation of towed decoy situation is deduced in this paper. Compared with the above literatures, the innovation points of this paper are as follows: 1) A new guidance strategy is proposed based on heading angle method and parallel approaching method. That the trajectory of guidance is above the towed decoy by a suitable angle is guaranteed by heading angle method. Meanwhile, the accurate interception of missiles to targets is guaranteed by parallel approaching method. 2) Compared to [14, 15], not only the input saturation problem is considered, but also a guidance law against towed decoys based on back-stepping sliding mode method is proposed. 3) Compared to [25–27], the two adaptive back-stepping sliding mode guidance laws converge much faster and a new type of auxiliary system is proposed.

The structure of this paper is as follows: Firstly, the system model with towed decoy is derived. Then, based on back-stepping sliding mode method, an adaptive back-stepping sliding mode controller is given, which makes the system state converges to an equilibrium point in finite time. Furthermore, in order to solve input saturation problems, an anti-saturation controller is given using adaptive and back-stepping sliding mode methods, with the help of an auxiliary system. And the state parameters of the system are asymptotically stable. Finally, a strict proof is given using Lyapunov stability theory, and the effectiveness of these two guidance laws is validated through numerical simulation.

2. DESRIPTION OF SYSTEM MODEL

In two dimension surface, the missile-target relative movement with towed disturbance is as shown in Fig. 1. Missile, target and towed decoy are treated as mass equilibrium and denoted by M, T and $TRAD$. The connecting line from missile to target is the line of sight. The other parameters are shown in the Fig. 1.

As shown in Fig. 1, r is the relative distance between missile and target. L is the length of towed line which can be given by radar or set as typical value from experience. q is the line of sight angle, which is the angle between line of sight and horizontal line. q_{TRAD} is the line of sight angle of towed decoy. Δq is the difference between q_{TRAD} and q. φ_M and φ_T are the angles of velocity direction. θ_M and θ_T are the leading angles of missile and target. V_M and V_T are the velocities of missile and target.

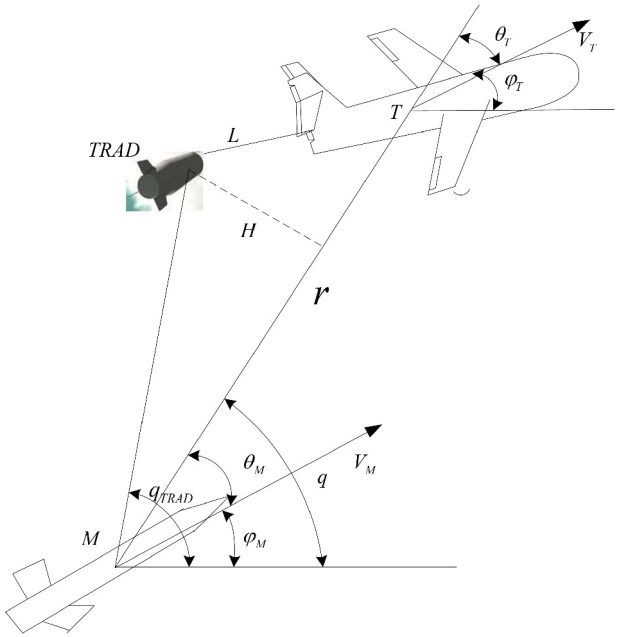

Fig. 1. The relative movement with towed decoy.

Suppose that the longitudinal velocities of missile and target are a constant respectively. Based on the geometrical relationship shown in Fig. 1, the relative movement can be described as shown below differential equations:

$$\Delta q \cdot r = L\sin\theta_T, \tag{1}$$
$$q = q_{TRAD} - \Delta q, \tag{2}$$
$$\theta_M = q_{TRAD} - \Delta q - \varphi_M, \tag{3}$$
$$\theta_T = q_{TRAD} - \Delta q - \varphi_T, \tag{4}$$
$$\dot{r} = V_T\cos\theta_T - V_M\cos\theta_M, \tag{5}$$
$$r\dot{q} = -V_T\sin\theta_T + V_M\sin\theta_M. \tag{6}$$

According to (1), one obtains

$$\Delta q = \frac{L\sin\theta_T}{r}. \tag{7}$$

Computing the first order derivative of (7), combining (6), leads to

$$\Delta\dot{q} = \frac{L\dot{\theta}_T\cos\theta_T}{r} - L\dot{r}\frac{V_M\sin\theta_M}{r^2V_t} + \frac{L\dot{r}}{rV_t}\dot{q}. \tag{8}$$

Computing the derivative of (6)

$$\begin{aligned}\dot{r}\dot{q} + r\ddot{q} = &-\dot{V}_T\sin\theta_T - V_T\cos\theta_T(\dot{q}-\dot{\varphi}_T)\\ &+\dot{V}_M\sin\theta_M + V_M\cos\theta_M(\dot{q}-\dot{\varphi}_M).\end{aligned} \tag{9}$$

Furthermore, equation (9) can be rewritten as

$$\ddot{q} = -\frac{2\dot{r}}{r}\dot{q} - \frac{a_M}{r} + g(t), \tag{10}$$

where $a_T = V_T\dot{\varphi}_T\cos\theta_T$ and $a_M = V_M\dot{\varphi}_M\cos\theta_M$ are the normal components of acceleration of missile. $g(t)$ is target's normal accelerations, during designing the guidance law and regarded as the system's unknown external disturbance input.

Based on leading angle method and parallel approaching guidance theory, if angle Δq and line of sight rate $\dot{q}$ satisfy

$$\begin{cases}\lim\limits_{t\to t_f}\Delta q(t) = 0,\\ \lim\limits_{t\to t_f}\dot{q}(t) = 0.\end{cases} \tag{11}$$

The accurate interception of missile and target will be guaranteed, where t_f is the interception time.

Remark 1: In [29], the trajectory of guidance is above the towed decoy by a suitable angle is guaranteed by heading angle method. Meanwhile, the accurate interception of missiles to targets is guaranteed by parallel approaching method [20].

In order to satisfy the requirement of interception control, let $x_1 = \Delta q(t)$ and $x_2 = \dot{q}(t)$ as state variables, combining (8) and (10), one obtains

$$\dot{x}_1 = F + \frac{L\dot{r}}{rV_t}x_2, \tag{12}$$

$$\dot{x}_2 = -\frac{2\dot{r}}{r}x_2 - \frac{1}{r}u + d, \tag{13}$$

where $F = \frac{L\dot{\theta}_T\cos\theta_T}{r} - L\dot{r}\frac{V_M\sin\theta_M}{r^2V_T}$, $u = a_M$ is the input of control, $d = g(t)$ is the unknown disturbance of system.

Remark 2: As is restrained by acceleration capability, the maximum lateral acceleration that can be actually provided by the missile and the target is limited. Thus, d is bounded.

In the terminal guidance stage, subject to the limitation of the power of angle tracking system of seeker and overload of receiver. According to [11], there is a minimum working distance r_0 for the seeker. When the relative distance between the missile and the target is less or equal to r_0, the inertial flying of missile in the guidance process is ended. Without loss of generality, the beginning time of terminal guidance is set as 0. For the convenience of guidance law design, the following assumption is given.

Assumption 1: There exists an unknown upper bound of disturbance d in the system model (13). That is, there is a positive constant d_M which satisfies

$$|d| \le d_M. \tag{14}$$

3. DESIGN OF CONTROLLERS

Considering system models (12)-(13), the problems of uncertainty and input saturation of the system, an adaptive back-stepping sliding mode controller and an adaptive back-stepping sliding mode saturation controller are designed using sliding mode, back-stepping and adaptive methods in this paper.

Lemma 1 [11]**:** For $x_i \in \mathrm{R}$, $i = 1, ..., n$, $0 < p \le 1$ is real number, then the following inequality holds

$$(|x_1| + \cdots + |x_n|)^p \le |x_1|^p + \cdots + |x_n|^p. \tag{15}$$

Lemma 2 [28]**:** Consider the system in (16), Suppose that there exists a Lyapunov function $V(x)$, scalars $\rho \in (0,1)$, $\alpha > 0$, and $0 < \sigma < \infty$, such that $\dot{V}(x) \le -\alpha V^\rho(x) + \sigma$. Then, we define the trajectory of this system as practical finite-time stability (PFTS).

$$\dot{x} = f(x(t)),\ x(0) = 0,\ f(0) = 0,\ x \in R. \tag{16}$$

3.1. Controller design based on back-stepping sliding mode and adaptive methods

Suppose that the upper bound of external disturbance d is unknown. An adaptive back-stepping sliding mode finite time controller is obtained using back-stepping sliding mode control theory and adaptive algorithm. The specific process is as follows:

In order to facilitate to design a finite time controller using back-stepping method, let

$$z_1 = x_1, \tag{17}$$

$$z_2 = x_2 - x_2^v. \tag{18}$$

Referring to [11], the virtual controller can be obtained as

$$x_2^v = -\frac{rV_t}{L\dot{r}}\left(F + k_1 x_1 + k_2 f(x_1)\right), \tag{19}$$

$$f(x_1) = \begin{cases} \dfrac{r_1}{\alpha_0}\left(e^{\alpha_0|x_1|} - 1\right)\operatorname{sign}(x_1) \\ \quad + r_2 \operatorname{sign}(x_1) x_1^2, & |x_1| \le \eta, \\ \operatorname{sig}(x_1)^\gamma, & \text{otherwise}, \end{cases} \tag{20}$$

$$r_1 = (2-\gamma)\eta^{\gamma-1}, \tag{21}$$

$$r_2 = (\gamma-1)\eta^{\gamma-2}, \tag{22}$$

where $0 < \gamma < 1$, α, β, k_1, k_2 and η are positive constants respectively.

Proposition 1: Using virtual controller (19), then state variable x_1 in (12) converges to 0 in finite time.

Proof: Choose the Lyapunov function as

$$V_1 = \frac{1}{2}x_1^2. \tag{23}$$

Computing the first order derivative of (23), combining (17) and (19), yield

$$\begin{aligned} \dot{V}_1 =& x_1\dot{x}_1 \\ & - x_1(k_1 x_1 + k_2 f(x_1)) \\ & - k_1 x_1^2 - k_2 x_1 f(x_1). \end{aligned} \tag{24}$$

When $|x_1| > \eta$, according to (24)

$$\begin{aligned} \dot{V}_1 &= -k_1 x_1^2 - k_2 x_1 \operatorname{sig}(x_1)^\gamma \\ &\le -2k_1 V_1 - 2^{(\gamma+1)/2} k_2 V_1^{(\gamma+1)/2}. \end{aligned} \tag{25}$$

When $|x_1| \le \eta$, according to (24)

$$\begin{aligned} \dot{V}_1 =& -k_1 x_1^2 - k_2 \frac{r_1}{\alpha_0}\left(e^{\alpha_0|x_1|} - 1\right)|x_1| \\ & - k_2 r_2 x_1 \operatorname{sign}(x_1) x_1^2 \\ =& -k_1 x_1^2 - k_2 \frac{r_1}{\alpha_0}\left(e^{\alpha_0|x_1|} - 1\right)|x_1| - k_2 r_2 |x_1| x_1^2 \\ \le& -2k_1 V_1. \end{aligned} \tag{26}$$

The above proof shows that x_1 converges to 0 in finite time. □

To guarantee the whole closed-loop system converges in finite time, choose sliding mode surface as

$$s = z_2. \tag{27}$$

To deal with time varying disturbance d with unknown upper bound, discontinuous finite time controller (28)-(29) is given in this paper, where k_3, k_4, h and p are positive constants. d satisfies $d \le d_M$, d_M is an unknown positive constant, and $\hat{d}_M$ is the estimated value of d_M, $\tilde{d}_M = d_M - \hat{d}_M$. Inspired by [11], the adaptive back-stepping sliding mode controller is given by

$$u = -2\dot{r}x_2 + \frac{L\dot{r}}{V_t}x_1 + r\left(\dot{x}_2^v + k_3 s + \left(k_4 + \hat{d}_M\right)\operatorname{sign}(s)\right), \tag{28}$$

$$\dot{\hat{d}}_M = p|s| - h\hat{d}_M. \tag{29}$$

Remark 3: In theory, s and $\dot{\hat{d}}_M$ will converge to zero in finite time. However, in practice, as the right-hand side of $\dot{\hat{d}}_M$ in (29) could be strictly positive for all time, $\dot{\hat{d}}_M$ may grow without bound. We can use $\dot{\hat{d}}_M = p|s| - h\hat{d}_M$ to replace (29) to deal with the problem practically, where p and h are positive constants.

Theorem 1: In the case that d is bounded but the upper boundary is unknown in the system (12)-(13), the following conclusions can be obtained using the adaptive back-stepping sliding mode controller (28)-(29).

1) There exists an upper bound of adaptive parameter$\hat{d}_M$, and there is a positive constant $\bar{d}_M$ satisfying $\hat{d}_M \le \bar{d}_M$.

2) Sliding mode manifold s converges to 0 in finite time.

3) State variables x_1 and z_2 of system converge to 0 in finite time.

Proof: Choose the Lyapunov function as

$$V_2 = \frac{1}{2}x_1^2 + \frac{1}{2}s^2 + \frac{1}{2p}\tilde{d}_M^2. \tag{30}$$

Computing the first order derivative of V_2, substituting control law (28)-(29) into it yields

$$\begin{aligned} \dot{V}_2 =& \dot{x}_1 + s\dot{s} - \frac{1}{p}\tilde{d}_M\dot{\hat{d}}_M \\ =& x_1\left(F + \frac{L\dot{r}}{rV_t}\left(s + x_2^v\right)\right) + s\left(\dot{x}_2 - \dot{x}_2^v\right) - \frac{1}{p}\tilde{d}_M\dot{\hat{d}}_M \\ & + s\left(-\frac{2\dot{r}}{r}x_2 - \frac{1}{r}u + d - \dot{x}_2^v\right) - \frac{1}{p}\tilde{d}_M\dot{\hat{d}}_M \\ \le& -k_1 x_1^2 - k_2 x_1 f(x_1) - k_3 s^2 - k_4 \operatorname{sign}(s) s \\ & + \frac{h}{p}\left(d_M - \hat{d}_M\right)\hat{d}_M \\ \le& -k_1 x_1^2 - k_2 x_1 f(x_1) - k_3 s^2 - k_4 \operatorname{sign}(s) s \\ & - \frac{1}{p}\left(d_M - \hat{d}_M\right)^2 + \frac{1}{p}\left(d_M - \hat{d}_M\right)^2 \\ & + \frac{1}{p}\left(d_M - \hat{d}_M\right)h\hat{d}_M \\ \le& -k_1 x_1^2 - k_2 x_1 f(x_1) - k_3 s^2 - k_4 \operatorname{sign}(s) s \\ & + \frac{1}{p}\left(d_M - \hat{d}_M\right)\left(d_M + (h-1)\hat{d}_M\right) \\ & - \frac{1}{p}\left(d_M - \hat{d}_M\right)^2 \\ \le& -k_1 x_1^2 - k_2 x_1 f(x_1) - k_3 s^2 - k_4 \operatorname{sign}(s) s \\ & - \frac{1}{p}\left[-(h-1)\hat{d}_M^2 + (h-2)d_M\hat{d}_M + d_M^2\right] \end{aligned}$$

$$-\frac{1}{p}\left(d_M-\hat{d}_M\right)^2. \tag{31}$$

Case 1: If $|x_1|>\eta$, equation (31)can be written as

$$\begin{aligned}\dot{V}_2\leq&-k_1x_1^2-k_2x_1\,\mathrm{sig}(x_1)^\gamma-k_4\mathrm{sign}(s)s-\frac{1}{p}\left(d_M-\hat{d}_M\right)^2\\&-k_3s^2-\frac{1}{p}\left[-(h-1)\,\hat{d}_M^2+(h-2)\,d_M\hat{d}_M+d_M^2\right]\\\leq&-k_1x_1^2-k_3s^2-\frac{1}{p}\left(d_M-\hat{d}_M\right)^2\\&-\frac{1}{p}\left[-(h-1)\,\hat{d}_M^2+(h-2)\,d_M\hat{d}_M+d_M^2\right].\end{aligned} \tag{32}$$

Case 2: If $|x_1|\leq\eta$, equation (31) can be written as

$$\begin{aligned}\dot{V}_2\leq&-k_2x_1\left(\frac{r_1}{\alpha_0}\left(e^{\alpha_0|x_1|}-1\right)\mathrm{sign}\,(x_1)+r_2\,\mathrm{sign}(x_1)x_1^2\right)\\&-k_1x_1^2-k_3s^2-k_4\mathrm{sign}(s)s-\frac{1}{p}\left(d_M-\hat{d}_M\right)^2\\&-\frac{1}{p}\left[-(h-1)\,\hat{d}_M^2+(h-2)\,d_M\hat{d}_M+d_M^2\right]\\\leq&-k_1x_1^2-k_3s^2-\frac{1}{p}\left(d_M-\hat{d}_M\right)^2\\&-\frac{1}{p}\left[-(h-1)\,\hat{d}_M^2+(h-2)\,d_M\hat{d}_M+d_M^2\right].\end{aligned} \tag{33}$$

According to (32) and (33)

$$\dot{V}_2\leq-\Pi\dot{V}_2+\frac{h^2d_M^2}{4p(h-1)}, \tag{34}$$

where $\Pi=\min\{2k_1,2k_3,2\}$, and the maximum values of $-\frac{1}{p}\left[-(h-1)\,\hat{d}_M^2+(h-2)\,d_M\hat{d}_M+d_M^2\right]$ is $\frac{h^2d_M^2}{4p(h-1)}$.

According to (34), V_2 is not increasing, and s and $\tilde{d}_M$ are bounded. Furthermore, $\hat{d}_M$ is bounded.

Then conclusion 1) is obtained.

Choose Lyapunov function as

$$V_3=\frac{1}{2}x_1^2+\frac{1}{2}s^2+\frac{1}{p}(\bar{d}_M-\hat{d}_M)^2, \tag{35}$$

where $\bar{d}_M$ is a positive constant and satisfies $\bar{d}_M>\hat{d}_M$ and $\bar{d}_M>d_M$.

Computing the derivative of V_3

$$\begin{aligned}\dot{V}_3=&\dot{x}_1+s\dot{s}-\frac{2}{p}(\bar{d}_M-\hat{d}_M)\dot{\hat{d}}_M\\=&-k_1x_1^2-k_2x_1f\,(x_1)+x_1s\\&+s\left(-\frac{2\dot{r}}{r}x_2-\frac{1}{r}u+d-\dot{x}_2^v\right)-\frac{2}{p}(\bar{d}_M-\hat{d}_M)\dot{\hat{d}}_M.\end{aligned} \tag{36}$$

Substituting control law (28)-(29) into (36), leads to

$$\begin{aligned}\dot{V}_3=&\dot{x}_1+s\dot{s}-\frac{2}{p}(\bar{d}_M-\hat{d}_M)\left(p\,|s|-h\hat{d}_M\right)\\\leq&-k_1x_1^2-k_2x_1f\,(x_1)-k_3s^2-k_4\,|s|-|s|\,(\bar{d}_M-\hat{d}_M)\\&+\frac{2}{p}(\bar{d}_M-\hat{d}_M)h\hat{d}_M\\\leq&-k_1x_1^2-k_2x_1f\,(x_1)-k_3s^2-k_4\,|s|-(\bar{d}_M-\hat{d}_M)\,|s|\\&+\frac{h}{2p}\bar{d}_M^2.\end{aligned} \tag{37}$$

To analyze the convergence problem of sliding mode, the problem is divided into the following six situations to discuss.

Case 1: If $|x_1|>\eta$ and $s\neq0$, equation (37) can be written as

$$\begin{aligned}\dot{V}_3\leq&-k_1x_1^2-k_2x_1f\,(x_1)-k_3s^2-k_4\,|s|\\&-(\bar{d}_M-\hat{d}_M)\,|s|+\frac{h}{2p}\bar{d}_M^2\\\leq&-k_1x_1^2-k_2x_1\,\mathrm{sig}(x_1)^\gamma-k_3s^2-k_4\,|s|\\&-(\bar{d}_M-\hat{d}_M)\,|s|+\frac{h}{2p}\bar{d}_M^2\\\leq&-\min(2^{(1+\gamma)/2}k_2,|s|^{1/2})\min(V_3^{(1+\gamma)/2},V_3^{1/2})\\&+\frac{h}{2p}\bar{d}_M^2.\end{aligned} \tag{38}$$

Case 2: If $|x_1|>\eta$ and $s\equiv0$, equation (37) can be written as

$$\begin{aligned}\dot{V}_3\leq&-k_1x_1^2-k_2x_1\,\mathrm{sig}(x_1)^\gamma-k_3s^2-k_4\,|s|\\&-(\bar{d}_M-\hat{d}_M)\,|s|+\frac{h}{2p}\bar{d}_M^2\\\leq&-k_1x_1^2-k_2x_1\,\mathrm{sig}(x_1)^\gamma+\frac{h}{2}\bar{d}_M^2\\\leq&-2k_1V_3+\frac{h}{2p}\bar{d}_M^2.\end{aligned} \tag{39}$$

According to (39) and Proposition 1, system variable x_1 converges to 0 in finite time.

Case 3: If $|x_1|>\eta$ and $s\not\equiv0$, substitute controller (28) into (13)

$$\dot{x}_2=\frac{L\dot{r}}{rV_t}x_1-\left(\dot{x}_2^v+k_3s+\left(k_4+\hat{d}_M\right)\mathrm{sign}(s)\right)+d\neq0. \tag{40}$$

So when $s\not\equiv0$, $\dot{x}_2$ is not an attractor. It can be guaranteed that the sliding mode manifold s converges to 0 in finite time.

Case 4: If $|x_1|\leq\eta$ and $s\neq0$, equation (37) can be rearranged as

$$\begin{aligned}\dot{V}_3=&-k_1x_1^2-k_2\frac{r_1}{\alpha_0}\left(e^{\alpha_0|x_1|}-1\right)|x_1|-k_2r_2\,\mathrm{sign}(x_1)x_1^2\\&-k_3s^2-k_4\,|s|-(\bar{d}_M-\hat{d}_M)\,|s|+\frac{h}{2p}\bar{d}_M^2\\\leq&-k_1x_1^2-k_2r_2\,\mathrm{sign}(x_1)x_1^2-k_3s^2-k_4\,|s|\end{aligned}$$

$$
\begin{aligned}
&-(\bar{d}_M-\hat{d}_M)|s|+\frac{h}{2p}\bar{d}_M^2\\
\le&-\min(2^{(1+\gamma)/2}k_2r_2,|s|^{1/2})\min(V_3^{(1+\gamma)/2},V_3^{1/2})\\
&+\frac{h}{2p}\bar{d}_M^2. \qquad (41)
\end{aligned}
$$

Case 5: If $|x_1|\le\eta$ and $s\equiv 0$,

$$
\begin{aligned}
\dot{V}_3=&-k_1x_1^2-k_2\frac{r_1}{\alpha_0}\left(e^{\alpha_0|x_1|}-1\right)|x_1|-k_2r_2\,\mathrm{sign}(x_1)x_1^2\\
&-k_3s^2-k_4|s|-(\bar{d}_M-\hat{d}_M)|s|+\frac{h}{2}\bar{d}_M^2\\
\le&-k_1x_1^2-k_2r_2\,\mathrm{sign}(x_1)x_1^2+\frac{h}{2}\bar{d}_M^2\\
\le&-(2^{(1+\gamma)/2}k_2r_2)V_3^{(1+\gamma)/2}+\frac{h}{2}\bar{d}_M^2. \qquad (42)
\end{aligned}
$$

According to (42) and Proposition 1, system variable x_1 converges to 0 in finite time.

Case 6: If $|x_1|\le\eta$ and $s\not\equiv 0$, substitute controller (28) into (13)

$$
\dot{x}_2=\frac{L\dot{r}}{rV_t}x_1-\left(\dot{x}_2^v+k_3s+\left(k_4+\hat{d}_M\right)\mathrm{sign}(s)\right)+d\neq 0. \qquad (43)
$$

So $s\not\equiv 0$, and s is not an attractor, and that the sliding mode manifold converges to 0 in finite time can be guaranteed.

From all above, the closed-loop system converges in finite time. Furthermore, sliding mode manifold s and x_1 converge to 0 in finite time as well.

So conclusion 2) is obtained.

Since sliding mode manifold s and x_1 converge in finite time, according to (27), z_2 converges to 0 in finite time. Then conclusion 3) is proved.

Therefore, the whole proof of Theorem 1 is completed. □

3.2. Design of anti-saturation controller based on bask-stepping sliding mode and adaptive methods

The saturation problem is not taken into consideration in controller (28), but the limitation of missile load is an important influence factor on controller, which could even cause the instability of the system. In order to solve this problem, an auxiliary system is built to deal with input saturation. Considering that the upper bound of time variable disturbance is unknown, an anti-saturation controller is proposed based on back-stepping sliding mode and adaptive methods.

Suppose the constraints of input saturation are

$$
u=\begin{cases}u_{\max}, & u_c\ge u_{\max},\\ u_c, & u_{\min}<u_c<u_{\max},\\ u_{\min}, & u_c\le u_{\min},\end{cases} \qquad (44)
$$

where, u is the desired control input, $u_{\max}$ and $u_{\min}$ are the maximum and minimum of control inputs respectively.

To deal with input saturation, the aim auxiliary system (45) is built up, with the reference of [19].

$$
\dot{\eta}_V=\begin{cases}-k_\eta\eta_V-\dfrac{1}{\|\eta_V\|^2}\left(|s\Delta u|+0.5\Delta u^2\right)\eta_V\\ \quad -\Delta u\eta_V-k_6\,\mathrm{sig}^\gamma(\eta_V), & \|\eta_V\|\geqslant\sigma_V,\\ 0, & \|\eta_V\|<\sigma_V,\end{cases} \qquad (45)
$$

where η_V is the state variable of the auxiliary system. δ_V, k_η and k_6 are positive constants, $\Delta u=u-u_c$.

To deal with the problem that the upper bound of disturbance is unknown and the constraint of input saturation, the anti-saturation controller based on back-stepping sliding mode and adaptive methods is given by

$$
\begin{aligned}
u_c=&r\left((k_4+\hat{d}_M)\mathrm{sign}(s)-k_5\eta_V+\frac{s\mu_V(s)}{\psi_V^2+\|s\|^2}\right)\\
&-2\dot{r}x_2+\frac{L\dot{r}}{V_t}x_1+r\left(\dot{x}_2^v+k_3s\right), \qquad (46)
\end{aligned}
$$

where $\mu_V(s)=0.5k_5^2s^2$.

And

$$
\dot{\psi}_V=\begin{cases}-k_V\psi_V-\dfrac{\mu_V(s)\psi_V}{\psi_V^2+\|s\|^2}+k_7\,\mathrm{sign}(\psi_V),\\ \qquad\qquad\qquad\qquad \|s\|\geqslant\psi_\varphi,\\ 0, \qquad\qquad\qquad\qquad \|s\|<\psi_\varphi,\end{cases} \qquad (47)
$$

$$
\dot{\hat{d}}_M=p|s|-h\hat{d}_M, \qquad (48)
$$

where k_V, Ψ_ϕ and k_7 are positive constants.

Theorem 2: For the system (12)-(13), if Assumption 1 is satisfied, the following conclusions can be draw using controller (46).

1) There exists an upper bound of adaptive parameter$\hat{d}_M$, and there is a positive constant $\bar{d}_M$ satisfying$\hat{d}_M\le\bar{d}_M$.

2) Sliding mode surface s is practical finite-time stable.

3) State parameters x_1 and z_2 of system are practical finite-time stable.

Proof: Adopt method similar to conclusion 1) in Theorem1 to obtain: adaptive parameter $\hat{d}_M$, and there is a positive constant $\bar{d}_M$ satisfying $\hat{d}_M\le\bar{d}_M$.

So conclusion 1) is obtained.

Choose Lyapunov function as

$$
V_4=\frac{1}{2}x_1^2+\frac{1}{2}s^2+\frac{1}{p}\left(\bar{d}_M-\hat{d}_M\right)^2+\frac{1}{2}\psi_V^2+\frac{1}{2}\eta_V^2. \qquad (49)
$$

Computing the derivative of V_4 along system (12)-(13), one obtains

$$
\dot{V}_4=x_1\left(F+\frac{L\dot{r}}{rV_t}(s+x_2^v)\right)+s(\dot{x}_2-\dot{x}_2^v)
$$

$$
\begin{aligned}
&-\frac{2}{p}\left(\bar{d}_M-\hat{d}_M\right)\dot{\hat{d}}_M+\psi_V\dot{\psi}_V+\eta_V\dot{\eta}_V\\
=&\frac{L\dot{r}}{rV_t}x_1s+x_1\left(F+\frac{L\dot{r}}{rV_t}\left(-\frac{rV_t}{L\dot{r}}\left(F+k_1x_1+k_2f(x_1)\right)\right)\right)\\
&+s\left(-\frac{2\dot{r}}{r}x_2-\frac{1}{r}u+d-\dot{x}_2^v\right)-\frac{2}{p}\left(\bar{d}_M-\hat{d}_M\right)\dot{\hat{d}}_M\\
&+\psi_V\dot{\psi}_V+\eta_V\dot{\eta}_V\\
=&-k_1x_1^2-k_2x_1f(x_1)+\frac{L\dot{r}}{rV_t}x_1s\\
&+s\left(-\frac{2\dot{r}}{r}x_2-\frac{1}{r}u+d-\dot{x}_2^v\right)-\frac{2}{p}\left(\bar{d}_M-\hat{d}_M\right)\dot{\hat{d}}_M\\
&+\psi_V\dot{\psi}_V+\eta_V\dot{\eta}_V. \qquad (50)
\end{aligned}
$$

Substituting the virtual controller (19) and (45)-(47) into (47)

$$
\begin{aligned}
\dot{V}_4\le&-k_1x_1^2-k_2x_1f(x_1)-k_3s^2-k_4\mathrm{sign}(s)s-k_\eta\eta_V^2\\
&-k_\psi\psi_V^2-k_6\eta_V\,\mathrm{sig}^\gamma(\eta_V)-\psi_Vk_7\,\mathrm{sign}(\psi_V)\\
&+s\left(d-\hat{d}_M\right)-\frac{2}{p}\left(\bar{d}_M-\hat{d}_M\right)\dot{\hat{d}}_M+k_5\eta_Vs+s\Delta u\\
&-|s\Delta u|-\frac{1}{2}\Delta u^2-\eta_V\Delta u-\frac{s^2\mu_V(s)}{\psi_V^2+\|s\|^2}\\
&-\frac{\mu_V(s)\,\psi_V^2}{\psi_V^2+\|s\|^2}. \qquad (51)
\end{aligned}
$$

Substituting the adaptive algorithm (48) into (51), lead to

$$
\begin{aligned}
\dot{V}_4\le&-k_1x_1^2-k_2x_1f(x_1)-k_3s^2-k_4\mathrm{sign}(s)s\\
&-k_\eta\eta_V^2-k_\psi\psi_V^2-k_6\eta_V\,\mathrm{sig}^\gamma(\eta_V)\\
&-\psi_Vk_7\,\mathrm{sign}(\psi_V)-|s|\left(\bar{d}_M-\hat{d}_M\right)\\
&+\frac{2}{p}(\bar{d}_M-\hat{d}_M)h\hat{d}_M+k_5\eta_Vs+s\Delta u\\
&-|s\Delta u|-\frac{1}{2}\Delta u^2-\eta_V\Delta u-\frac{s^2\mu_V(s)}{\psi_V^2+\|s\|^2}\\
&-\frac{\mu_V(s)\,\psi_V^2}{\psi_V^2+\|s\|^2}. \qquad (52)
\end{aligned}
$$

Because of $s\Delta u-|s\Delta u|\le 0$, inequality (52) can be rewritten as

$$
\begin{aligned}
\dot{V}_4\le&-k_1x_1^2-k_2x_1f(x_1)-k_3s^2-k_4\mathrm{sign}(s)s\\
&-k_\eta\eta_V^2-k_\psi\psi_V^2-k_6\eta_V\,\mathrm{sig}^\gamma(\eta_V)\\
&-\psi_Vk_7\,\mathrm{sign}(\psi_V)+\frac{1}{p}\left(d_M-\hat{d}_M\right)h\hat{d}_M\\
&+k_5\eta_Vs-\frac{1}{2}\Delta u^2-\eta_V\Delta u-\frac{s^2\mu_V(s)}{\psi_V^2+\|s\|^2}\\
&-\frac{\mu_V(s)\left(\psi_V^2+s^2\right)-\mu_V(s)s^2}{\psi_V^2+\|s\|^2}\\
\le&-k_1x_1^2-k_2x_1f(x_1)-k_3s^2-k_4\mathrm{sign}(s)s-k_\eta\eta_V^2\\
&-k_\psi\psi_V^2-k_6\eta_V\,\mathrm{sig}^\gamma(\eta_V)-\psi_Vk_7\,\mathrm{sign}(\psi_V)\\
&-|s|\left(\bar{d}_M-\hat{d}_M\right)+\frac{2}{p}(\bar{d}_M-\hat{d}_M)h\hat{d}_M\\
&+k_5\eta_Vs-\frac{1}{2}\Delta u^2-\eta_V\Delta u-\mu_V(s). \qquad (53)
\end{aligned}
$$

Since

$$
k_5\eta_Vs-\eta_V\Delta u\le\frac{1}{2}k_5^2s^2+\eta_V^2+\frac{1}{2}\Delta u^2, \qquad (54)
$$

inequality (53) can be written as

$$
\begin{aligned}
\dot{V}_4\le&-k_1x_1^2-k_2x_1f(x_1)-k_3s^2-k_4\mathrm{sign}(s)s-k_\eta\eta_V^2\\
&-k_\psi\psi_V^2-k_6\eta_V\,\mathrm{sig}^\gamma(\eta_V)-\psi_Vk_7\,\mathrm{sign}(\psi_V)\\
&-|s|\left(\bar{d}_M-\hat{d}_M\right)+\frac{2}{p}(\bar{d}_M-\hat{d}_M)h\hat{d}_M\\
&+\frac{1}{2}k_5^2s^2+\eta_V^2-\mu_V(s). \qquad (55)
\end{aligned}
$$

Since $\mu_V(s)=0.5k_5^2s^2$, equation (55) can be rearranged as

$$
\begin{aligned}
\dot{V}_4\le&-k_1x_1^2-k_2x_1f(x_1)-k_3s^2-k_4\mathrm{sign}(s)s-k_\psi\psi_V^2\\
&-(k_\eta-1)\,\eta_V^2-k_6\eta_V\,\mathrm{sig}^\gamma(\eta_V)-\psi_Vk_7\,\mathrm{sign}(\psi_V)\\
&-|s|\left(\bar{d}_M-\hat{d}_M\right)+\frac{2}{p}(\bar{d}_M-\hat{d}_M)h\hat{d}_M. \qquad (56)
\end{aligned}
$$

If $x_1>\eta$, equation (56) can be rewritten as

$$
\begin{aligned}
\dot{V}_4\le&-k_1x_1^2-k_2x_1\,\mathrm{sig}(x_1)^\gamma-k_3s^2-k_4\mathrm{sign}(s)s\\
&-(k_\eta-1)\,\eta_V^2-k_\psi\psi_V^2-k_6\eta_V\,\mathrm{sig}^\gamma(\eta_V)\\
&-k_7\psi_V\,\mathrm{sign}(\psi_V)-|s|\left(\bar{d}_M-\hat{d}_M\right)\\
&+\frac{2}{p}(\bar{d}_M-\hat{d}_M)h\hat{d}_M\\
\le&-\min(2^{(1+\gamma)/2}k_2,|s|^{1/2},2^{(1+\gamma)/2}k_6,k_7^{1/2})\\
&\times\min(V_4^{(1+\gamma)/2},V_4^{1/2})+\frac{h}{2p}\bar{d}_M^2. \qquad (57)
\end{aligned}
$$

If $|x_1|\le\eta$, equation (56) can be written as

$$
\begin{aligned}
\dot{V}_4\le&-k_1x_1^2-k_2\frac{r_1}{\alpha_0}\left(e^{\alpha_0|x_1|}-1\right)\mathrm{sign}(x_1)x_1\\
&-k_2r_2\,\mathrm{sign}(x_1)x_1^2-k_3s^2-k_4\mathrm{sign}(s)s\\
&-(k_\eta-1)\,\eta_V^2-k_\psi\psi_V^2-k_6\eta_V\,\mathrm{sig}^\gamma(\eta_V)\\
&-k_7\psi_V\,\mathrm{sign}(\psi_V)-|s|\left(\bar{d}_M-\hat{d}_M\right)\\
&+\frac{2}{p}(\bar{d}_M-\hat{d}_M)h\hat{d}_M\\
\le&-k_1x_1^2-k_2r_2\,\mathrm{sign}(x_1)x_1^2-k_3s^2-|s|\left(\bar{d}_M-\hat{d}_M\right)\\
&-k_4\mathrm{sign}(s)s-(k_\eta-1)\,\eta_V^2-k_\psi\psi_V^2\\
&-k_6\eta_V\,\mathrm{sig}^\gamma(\eta_V)-k_7\psi_V\,\mathrm{sign}(\psi_V)\\
&+\frac{2}{p}(\bar{d}_M-\hat{d}_M)h\hat{d}_M
\end{aligned}
$$

$$\leq -\min(2^{(1+\gamma)/2}k_2 r_2, |s|^{1/2}, 2^{(1+\gamma)/2}k_6, k_7^{1/2}) \times \min(V_4^{(1+\gamma)/2}, V_4^{1/2}) + \frac{h}{2p}\bar{d}_M^2. \quad (58)$$

where $\phi(t) = k_1 x_1^2 + k_3 s^2 + (k_\eta - 1)\eta_V^2 + k_\psi \psi_V^2$, $k_\eta > 1$.

According to the above (54)-(55) and Lemma 2, it can be seen that the s is practical finite-time stable. So conclusion 2) in Theorem 2 is valid.

Since sliding mode manifold s and x_1 are practical finite-time stable, from (27) z_2 is also practical finite-time

Therefore, the whole proof of conclusion 3) in Theorem 2 is completed. □

Remark 4: The constrains (44) of input saturation and the controller (46) are represented by $k_5\eta_V$, mainly from the following two aspects:

If $\|\eta_V\| \geq \sigma_V > 0$, there exists input saturation:

(a) If $u_c \geq u_{\max}$, u_c decreases to $u_{\max}$ can be guaranteed by $k_5\eta_V$;

(b) If $u_c < u_{\min}$, u_c increases to $u_{\min}$ can be guaranteed by $k_5\eta_V$.

So, $u_c = u_{\max}$ or $u_c = u_{\min}$.

If $\|\eta_V\| < \sigma_V$ and $\dot{\eta}_V = 0$, then there is no input saturation. So $\Delta u = 0$. $u_{\min} < u_c < u_{\max}$ can be guaranteed by $k_5\eta_V$. So $u = u_c$.

4. SIMULATIONS

In order to verify the effectiveness of controllers (28)-(29) and controllers (45)-(48), we will carry out the following simulation.

4.1. Simulation analysis on adaptive back-stepping sliding mode controller

Assume that the flight speed of a certain type interception the Mach is 4.5, and velocity of sound is 295.07 m/s. The speed of the target is 700 m/s. The missile and target are moving in the vertical surface.

Suppose at the beginning of terminal guidance phase, the position of the missile in inertial coordinates is $x_m(0) = 0.5$ km, $y_m(0) = 16$ km. The initial trajectory deflection angle $\varphi_m(0)$ is 10°; similarly, the position of target is $x_t(0) = 12$ km, $y_t(0) = 17.5$ km. The initial trajectory deflection angle $\varphi_t(0)$ is 0°; the missile equips with an active radar seeker, and its dead zone is 100 m; the length L of towed decoy is 100 m; parameters in controller (28) are chosen as $k_1 = 100$, $k_2 = 70.5$, $k_3 = 0.003$, $k_4 = 0.003$, $\gamma = 0.85$, $h = 0.5$, $p = 0.8$, $\alpha_0 = 0.5$ and $\eta = 0.01$; normal acceleration of missile is set as $40g$, $g = 9.8$ m/s^2.

Suppose the measurement noise of line-of-sight rate is Gauss white noise with mean value 0 and variance 1×10^{-4}. The target is taking a cosine movement $a_{t\varepsilon} = 4g\cos(\pi t/4)$ in the direction vertical to line-of-sight.

For better illustration, the integral sliding mode guidance law (ISMGM) [16] is employed in simulations for performance comparison.

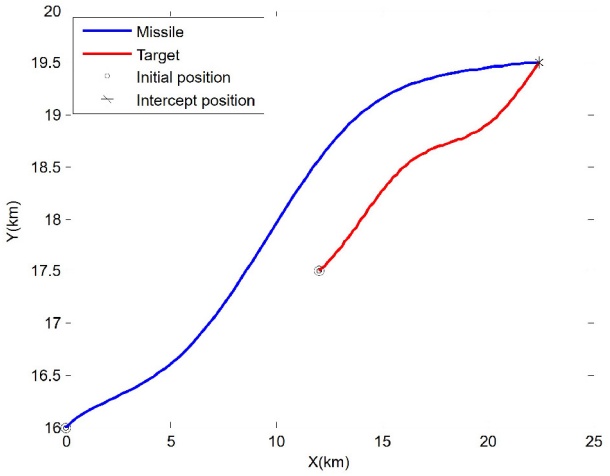

Fig. 2. Trajectories of missile and target.

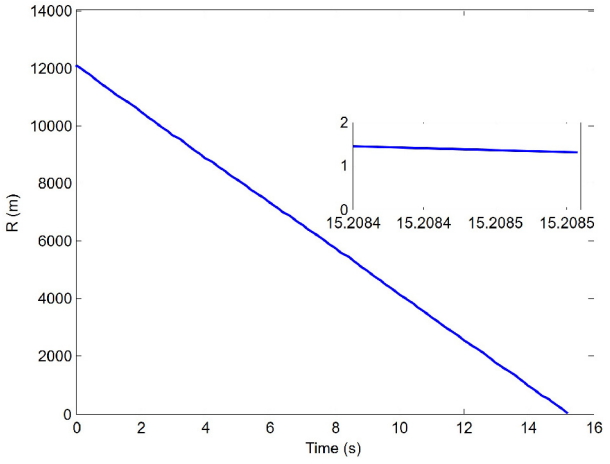

Fig. 3. 3The relative distance of missile and target.

Table 1. Miss distances and interception times.

Guidance law	Miss distance(m)	Interception time(s)
ISMGM	0.5428	15.67
ABSMC	0.1836	15.21

The simulation curves include the trajectories of missile and target, the relative distance of missile and target, the curve of line-of-sight angle rate, the curve of adaptive parameter obtained by adaptive back-stepping sliding mode controller (ABSMC) shown in Figs. 2-5. The curve of line-of-sight angle Δq, the curve of missile normal acceleration, obtained by ABSMC and ISGM are shown in Figs. 6-7. Table 1 presents the miss distances and interception times, obtained by these two different guidance laws.

From Fig. 2, it can see that the missile intercepts the target exactly in two-dimension surface. Fig. 3 shows that the interception time is 15.21 s and miss distance is 0.1836

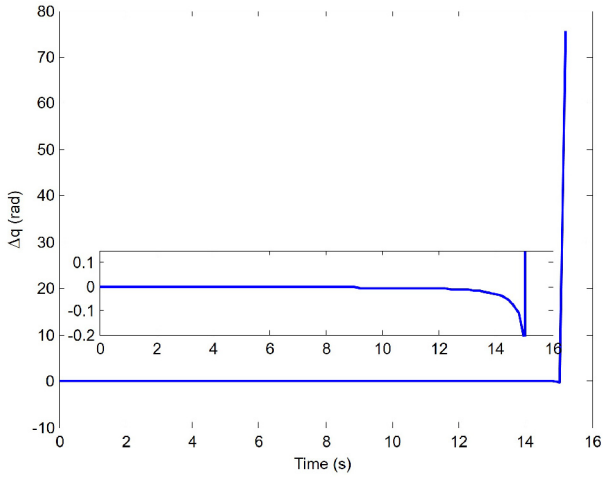

Fig. 4. Curve of line-of-sight angle Δq.

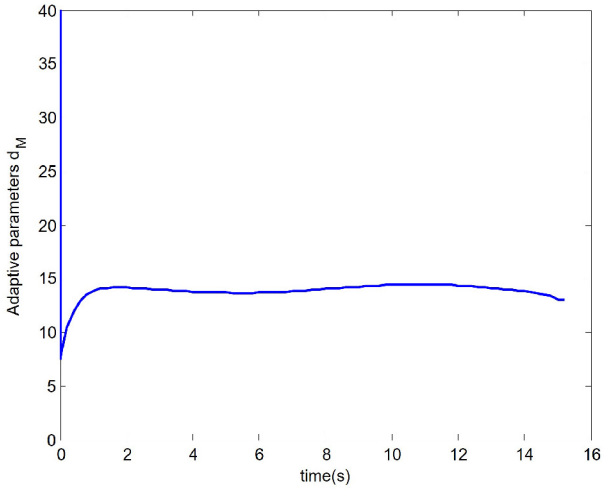

Fig. 5. Curve of adaptive parameter.

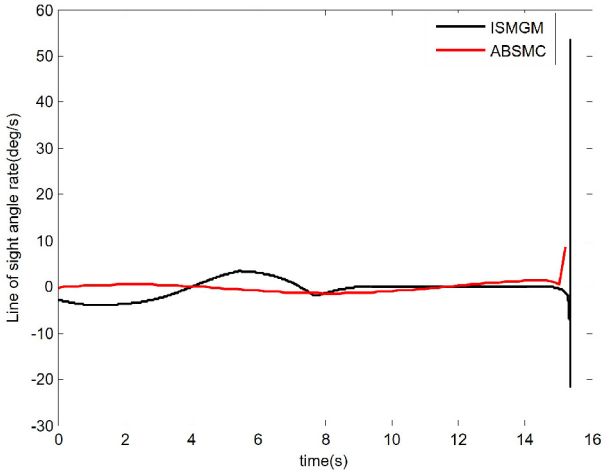

Fig. 6. Curve of line-of-sight angle rate.

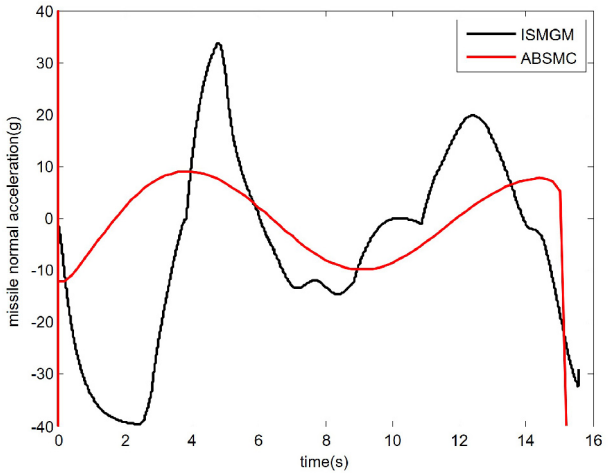

Fig. 7. Curve of missile normal acceleration.

m, which meet the requirement of high accuracy guidance. Fig. 4 depicts that the difference angle Δq approximately goes to zero. From Fig. 5, it can be seen that the adaptive parameters tend to steady-state values in short time. From the Fig. 6, it can be obtained the proposed ABSMC can ensure that the line-of-sight angular rate converge to a small neighourhood of zero rapidly in finite time for the two cases and they do not diverge until the last instant. ISGM diverges at an early time which leads to a large miss distance (see Table 1), so the guidance performance of the proposed ABSMC law is superior to that of ISGM. Fig.7 indicates that the acceleration commands under the proposed ABSMC law experience the occurrence of the saturation in the initial phase of the terminal guidance process with a smaller control gain compared with ISGM.

4.2. Simulation analysis on anti-saturation controller based on back-stepping sliding mode and adaptive methods

In order to verify the effectiveness of controller (45)-(48), we set the initial values of missile and target as same as those in 4.1 section. In order to test the robustness to the proposed control strategy, the simulation is divided into three cases of target acceleration as follows:

Case 1: Constant maneuvering $a_t = 4g$

Case 2: Cosine maneuvering $a_t = 4g\cos(\pi t/4)$

Case 3: Square wave maneuvering

$$a_t = 5g \cdot \mathrm{sign}(\sin(0.4\pi t)).$$

The guidance distance of seeker $r_0 = 100$ m. Parameters in controller are set as: $k_1 = 100$, $k_2 = 70.5$, $k_3 = 0.003$, $k_4 = 0.003$, $k_5 = 0.001$, $k_6 = 0.02$, $k_7 = 0.05$,$k_\eta = 1$, $\sigma_V = 0.1$, $k_\psi = 1$, $\psi_\phi = 0.01$, $\gamma = 0.85$, $h = 0.2$, $p = 1.2$, $\alpha_0 = 0.5$ and $\eta = 0.01$. Normal acceleration of missile is set as $40g$, $g = 9.8$ m/s^2. The simulation results are shown in Figs. 8-11 and Table 2.

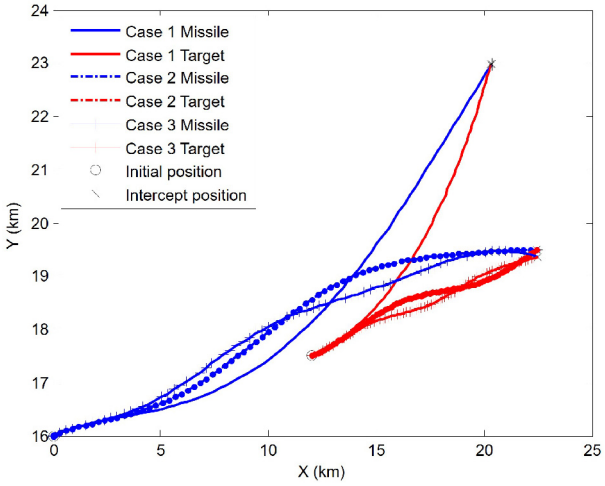

Fig. 8. Trajectories of missile and target.

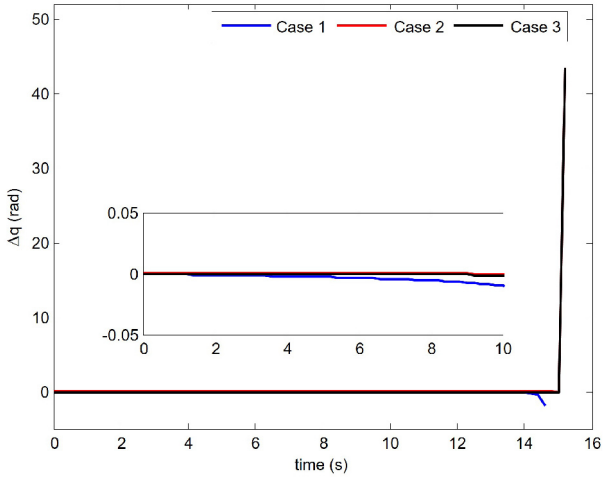

Fig. 9. Curve of line-of-sight angle Δq.

Table 2. Miss distances and interception times.

	Miss distance(m)	Interception time(s)
$a_t = 4g$	0.3836	14.86
$a_t = 4g\cos(\pi t/4)$	0.563	15.21
$a_t = 5g \cdot \text{sign}(\sin(0.4\pi t))$	0.746	15.41

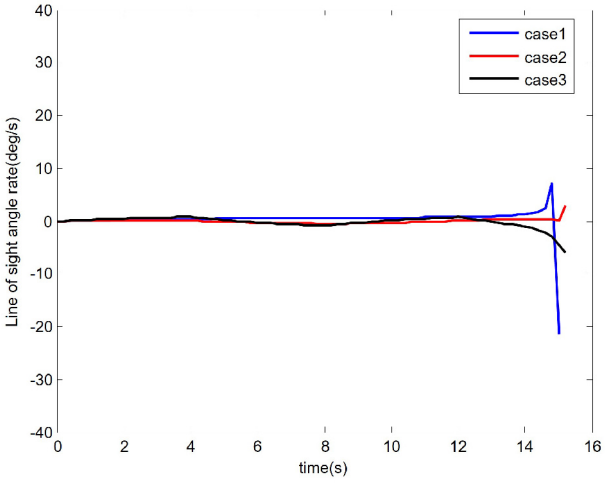

Fig. 10. Curve of line-of-sight angle rate.

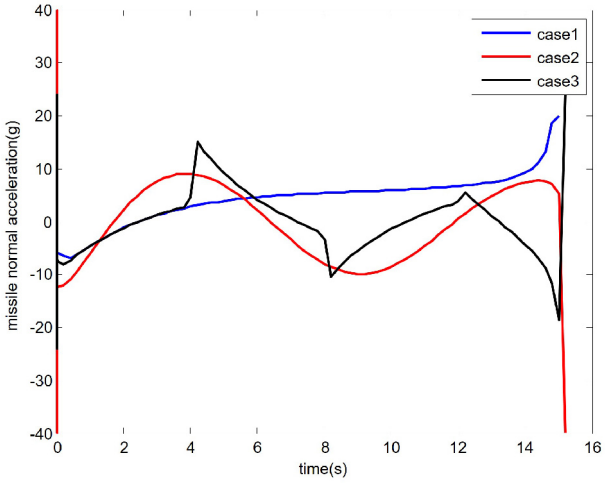

Fig. 11. Curve of missile normal acceleration.

It can be clearly observed from the Fig.8 that, with the implementation of the proposed controllers (45)-(48), the missile can intercept the target successfully for all the target acceleration profiles of Cases 1-3. From the Fig. 9, it shows that all Δq converges to zero in finite time, which guarantees the accuracy hit of missile to the target. From the Fig.10, it can be obtained that both proposed guidance laws can ensure that line-of-sight angle rates converge to zero in finite time for the target acceleration profiles of Cases 1-3. Fig. 11 shows the curves of the interception missile normal acceleration under three Cases 1-3. Because the influence derived from the dynamic delay of the automatic pilot in the missile does not be considered. The acceleration of the missile at a control-time point is larger. Fig.12 indicates the curves of the adaptive parameters in the controllers (45)-(48), revealing that after a period of time adaptive parameters tend to stable value. The miss distances and interception time achieved by the proposed controllers (45)-(48) for the three cases, respectively, (see Table 2).

5. CONCLUSION

Two guidance laws are proposed in this paper using sliding mode, back-stepping and adaptive method to deal with the guidance problem with towed decoy. Main conclusions are as followings:

1) Trajectory models of missile and target with towed decoy are given. And a new guidance strategy is pro-

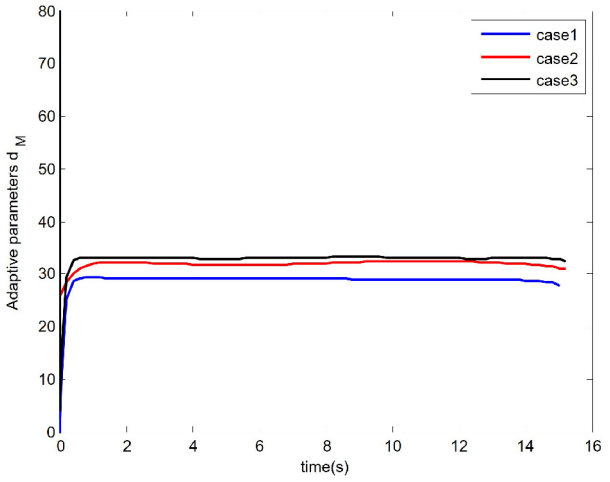

Fig. 12. Curve of adaptive parameter.

posed based on heading angle method and parallel approach method.

2) Considering unknown bounded system disturbance, a back-stepping sliding mode controller is given, which can guarantee the states of the system are stable in finite time. An anti-saturation controller is given using adaptive and back-stepping sliding mode methods, with the help of an auxiliary system. And the state variables of the system are asymptotically stable.

3) Strict proofs of the two controllers are given using Lyapunov theory. Simulation results have been presented to confirm the effectiveness of the proposed methods.

REFERENCES

[1] W. X. Bai, H Tian, and J. F. T, "Analysis of towed decoy jamming on monopulse radar," *Electronic Information Warfare Technology*, vol. 22, no. 6, pp. 39-42, 2007.

[2] W. J. Kerins. "Analysis of towed decoys," *IEEE transactions on aerospace and electronic systems*, vol. 29, no. 4, pp. 1222-1227, 1993.

[3] D.K. Barton, *Radar Evaluation Handbook*, Artech House, London, 1991.

[4] N. B. Benton, "Fiber optic microwave link applications in towed decoy electronic countermeasures systems," *Proc. of SPIE's 1995 International Symposium on Optical Science, Engineering, and Instrumentation. International Society for Optics and Photonics*, USA. pp. 85-92, July 1995.

[5] Y. L. Lu, Z. X. Tong, C. Z. Wang, and J. Jian, "Aerodynamic and dynamic characteristics of aeronautic towed decoy," *Journal of Beijing University of Aeronautics and Astronautics*, vol. 37, no. 4, pp. 395-398, 2011.

[6] W. D. Bai, A. F. Li, and S. B. Li, "Simulation and analysis of radar decoy jamming," *Electronic Information Warfare Technology*, vol. 23. no. 2, pp. 53-57, 2008.

[7] F. Neri, "Anti-monopulse jamming techniques," *Microwave and Optoelectronics Conference, 2001. IMOC 2001. Proceedings of the 2001 SBMO/IEEE MTT-S International*, IEEE, Belem, Brazil vol. 2, pp. 45-50, Aug. 2001.

[8] S. D. Brierley and R. Longchamp, "Application of sliding-mode control to air-air interception problem," *IEEE Transactions on Aerospace and Electronic Systems*, vol. 26, no. 2, pp. 306-325, 1990.

[9] A. Ilchmann and D. H. Owens, "Adaptive stabilization with exponential decay," *Systems & Control Letters*, vol. 14, no. 5, pp. 437-443, 1990.

[10] D. Y. N. Chavez and J. A. Moreno, "Second-order sliding mode output feedback controller with adaptation," *International Journal of Adaptive Control and Signal Processing*, vol. 30, no. 8-10, pp. 1523-1543, 2016.

[11] J. H. Song, S. M. Song, and H. B. Zhou, "Adaptive non-singular fast terminal sliding mode guidance law with impact angle constraints," *International Journal of Control, Automation and Systems*, vol. 14, no. 1, pp. 99-114, 2016.

[12] J. H. Song and S. M. Song, "Three-dimensional guidance law based on adaptive integral sliding mode control," *Chinese Journal of Aeronautics*, vol. 29, no. 1, pp. 202-214, 2016.

[13] Z. X. Zhang, S. H. Li, and S. Luo, "Composite guidance laws based on sliding mode control with impact angle constraint and autopilot lag," *Transactions of the Institute of Measurement and Control*, vol. 35, no. 6, pp. 764-776, 2013.

[14] D. Zhou, C. D. Mu, and W. Xu, "Fuzzy adaptive variable structure guidance with application to space interception," *Tsinghua Science and Technology*, vol. 4, no. 4, pp. 1610-1614, 1999.

[15] D. Zhou, C. D. Mu, and W. Xu, "Adaptive sliding-mode guidance of a homing missile," *Journal of Guidance, Control, and Dynamics*, vol. 22, no. 4, pp. 589-594. 1999.

[16] J. C. Holloway and M. Krstic, "A predictor observer for seeker delay in the missile homing loop," *Proc. of 12th IFAC Workshop on Time Delay Systems*, Ann Arbor, MI, USA, vol. 48, pp. 416-421, 2015.

[17] T. R. Oliveira, J. P. V. S. Cunha, and A. Battistel, "Global stability and simultaneous compensation of state and output delays for nonlinear systems via output-feedback sliding mode control," *Journal of Control, Automation and Electrical Systems*, vol. 27, no. 6, pp. 608-6202, 2016.

[18] S. Lee, Y. Kim, G. Moon, and B. E. Jun, "Adaptive back-stepping autopilot design for missiles of fast time-varying velocity," *IFAC-PapersOnLine*, vol. 49, no. 17, pp. 474-479, 2016.

[19] S. F. Xiong, W. H. Wang, X. D. Liu, S. Wang, and Z. Q. Chen, "Guidance law against maneuvering targets with intercept angle constraint," *ISA Transactions*, vol. 53, no. 4, pp. 1332-1342, 2014.

[20] M. Golestani, I. Mohammadzaman, and A. R .Vali, "Finite-time convergent guidance law based on integral backstepping control," *Aerospace Science and Technology*, vol.39, pp. 370-376. 2014.

[21] S. M. He, W. Wang, and J. Wang, "Three-dimensional multivariable integrated guidance and control design for maneuvering targets interception," *Journal of the Franklin Institute*, vol. 353, no. 16, pp. 4330-4350, 2016.

[22] X. L. Shao and H. J. Wang, "Back-stepping active disturbance rejection control design for integrated missile guidance and control system via reduced-order ESO," *ISA Transactions*, vol. 57, pp. 10-22, 2015.

[23] M. P. Ran, Q. Wang, D. H. Hou, and C. Y. Dong, "Back-stepping design of missile guidance and control based on adaptive fuzzy sliding mode control," *Chinese Journal of Aeronautics*, vol. 27, no. 3, pp. 634-642, 2014.

[24] M. Chen, S. S. Ge, and B. B. Ren, "Adaptive tracking control of uncertain MIMO nonlinear systems with input constraints," *Automatica*, vol. 47, no. 3, pp. 452-465, 2011.

[25] X. L. Liang, Z. H. Ming, and G. R. Duan, "Adaptive dynamic surface control for integrated missile guidance and autopilot in the presence of input saturation," *Journal of Aerospace Engineering*, vol. 28, no. 5, 2014.

[26] M. Chen, G. Tao, and B. Jiang, "Dynamic surface control using neural networks for a class of uncertain nonlinear systems with input saturation," *IEEE Transactions on Neural Networks and Learning Systems*, vol. 26, no. 9, pp. 2086-2097, 2015.

[27] D. Zhou and B Xu, "Adaptive dynamic surface guidance law with input saturation constraint and autopilot dynamics," *Journal of Guidance, Control, and Dynamics*, vol. 39, no. 1, pp. 1-8, 2016.

[28] Q. L. Hu, B. Jiang, and M. I. Friswell, "Robust saturated finite time output feedback attitude stabilization for rigid spacecraft," *Journal of Guidance, Control, and Dynamics*, vol. 37, no. 6, pp. 1914-1929, 2014.

[29] G. Y. Zhang, *Phased Array Radar Theory*, National Defence Industry Press, Beijing, 2009.

[30] Y. X. Zhang, M. W. Sun, and Z. Q. Chen, "Finite-time convergent guidance law with impact angle constraint based on sliding-mode control," *Nonlinear Dynamics*, vol. 70, no. 1, pp. 619-625, 2012.

JI-Peng Dong received his M.S. degrees in student in the School of Astronautics at Harbin Institute of Technology. His main research interests include sliding mode control and adaptive control, missile guidance and control systems.

Jing-Guang Sun received his M.S. degree in School of Automation from Harbin Engineering University he is a Ph.D. student in the School of Astronautics at Harbin Institute of Technology. His main research interests include Hypersonic Aircrafts control and nonlinear control.

Yong Guo received his Ph.D. degree in Control Science and Engineering from Harbin Institute of Technology in 2016. Currently, he is an assistant professor in the School of Automation at Northwestern Polytechnical University. His main research interests include spacecraft coordination control and nonlinear control.

Shen-Min Song received his Ph.D. degree in Control Theory and Application from Harbin Institute of Technology in 1996. He carried out postdoctoral research at Tokyo University from 2000 to 2002. He is currently a professor in the School of Astronautics at Harbin Institute of Technology. His main research interests include spacecraft guidance and control, intelligent control, and nonlinear theory and application.